Research Article | Vol. 25, No. 12 | 12 Jun 2017 | OPTICS EXPRESS 13883
Optics EXPRESS

Interferenceless coded aperture correlation holography–a new technique for recording incoherent digital holograms without two-wave interference

A. VIJAYAKUMAR* AND JOSEPH ROSEN

Department of Electrical and Computer Engineering, Ben-Gurion University of the Negev, P.O. Box 653, Beer-Sheva 8410501, Israel
physics.vijay@gmail.com

Abstract: Recording digital holograms without wave interference simplifies the optical systems, increases their power efficiency and avoids complicated aligning procedures. We propose and demonstrate a new technique of digital hologram acquisition without two-wave interference. Incoherent light emitted from an object propagates through a random-like coded phase mask and recorded directly without interference by a digital camera. In the training stage of the system, a point spread hologram (PSH) is first recorded by modulating the light diffracted from a point object by the coded phase masks. At least two different masks should be used to record two different intensity distributions at all possible axial locations. The various recorded patterns at every axial location are superposed in the computer to obtain a complex valued PSH library cataloged to its axial location. Following the training stage, an object is placed within the axial boundaries of the PSH library and the light diffracted from the object is once again modulated by the same phase masks. The intensity patterns are recorded and superposed exactly as the PSH to yield a complex hologram of the object. The object information at any particular plane is reconstructed by a cross-correlation between the complex valued hologram and the appropriate element of the PSH library. The characteristics and the performance of the proposed system were compared with an equivalent regular imaging system.

OCIS codes: (090.1995) Digital holography; (110.0110) Imaging systems; (090.1760) Computer holography; (050.5080) Phase shift; (050.0050) Diffraction and gratings; (110.0180) Microscopy.

References and links

1. G. Indebetouw, P. Klysubun, T. Kim, and T.-C. Poon, "Imaging properties of scanning holographic microscopy," J. Opt. Soc. Am. A **17**(3), 380–390 (2000).
2. J. Hong and M. K. Kim, "Single-shot self-interference incoherent digital holography using off-axis configuration," Opt. Lett. **38**(23), 5196–5199 (2013).
3. T. Yanagawa, R. Abe, and Y. Hayasaki, "Three-dimensional mapping of fluorescent nanoparticles using incoherent digital holography," Opt. Lett. **40**(14), 3312–3315 (2015).
4. M. K. Kim, "Adaptive optics by incoherent digital holography," Opt. Lett. **37**(13), 2694–2696 (2012).
5. J. Rosen, G. Brooker, G. Indebetouw, and N. T. Shaked, "A review of incoherent digital Fresnel holography," J. Hologr. Speckle **5**(2), 124–140 (2009).
6. J. W. Goodman, *Introduction to Fourier Optics* (McGraw-Hill, 1968), Chap. 9, pp. 295–313.
7. N. T. Shaked, B. Katz, and J. Rosen, "Review of three-dimensional holographic imaging by multiple-viewpoint-projection based methods," Appl. Opt. **48**(34), H120–H136 (2009).
8. T. Leportier and M. C. Park, "Generation of binary holograms for deep scenes captured with a camera and a depth sensor," Opt. Eng. **56**(1), 013107 (2017).
9. J. Rosen and G. Brooker, "Digital spatially incoherent Fresnel holography," Opt. Lett. **32**(8), 912–914 (2007).
10. P. Bouchal, J. Kapitán, R. Chmelík, and Z. Bouchal, "Point spread function and two-point resolution in Fresnel incoherent correlation holography," Opt. Express **19**(16), 15603–15620 (2011).
11. J. Rosen, N. Siegel, and G. Brooker, "Theoretical and experimental demonstration of resolution beyond the Rayleigh limit by FINCH fluorescence microscopic imaging," Opt. Express **19**(27), 26249–26268 (2011).
12. X. Lai, S. Zeng, X. Lv, J. Yuan, and L. Fu, "Violation of the Lagrange invariant in an optical imaging system," Opt. Lett. **38**(11), 1896–1898 (2013).

#291618 https://doi.org/10.1364/OE.25.013883
Journal © 2017 Received 28 Mar 2017; revised 9 May 2017; accepted 9 May 2017; published 9 Jun 2017

Optics EXPRESS

13. J. Rosen and R. Kelner, "Modified Lagrange invariants and their role in determining transverse and axial imaging resolutions of self-interference incoherent holographic systems," Opt. Express **22**(23), 29048–29066 (2014).
14. X. Lai, S. Xiao, Y. Guo, X. Lv, and S. Zeng, "Experimentally exploiting the violation of the Lagrange invariant for resolution improvement," Opt. Express **23**(24), 31408–31418 (2015).
15. Y. Kashter, A. Vijayakumar, Y. Miyamoto, and J. Rosen, "Enhanced super resolution using Fresnel incoherent correlation holography with structured illumination," Opt. Lett. **41**(7), 1558–1561 (2016).
16. R. Kelner, B. Katz, and J. Rosen, "Optical sectioning using a digital Fresnel incoherent-holography-based confocal imaging system," Optica **1**(2), 70–74 (2014).
17. R. Kelner and J. Rosen, "Parallel-mode scanning optical sectioning using digital Fresnel holography with three-wave interference phase-shifting," Opt. Express **24**(3), 2200–2214 (2016).
18. K.-H. Choi, J. Yim, and S.-W. Min, "Optical defocus noise suppressing by using a pinhole-polarizer in Fresnel incoherent correlation holography," Appl. Opt. **56**(13), F121–F127 (2017).
19. A. Vijayakumar, Y. Kashter, R. Kelner, and J. Rosen, "Coded aperture correlation holography-a new type of incoherent digital holograms," Opt. Express **24**(11), 12430–12441 (2016).
20. A. Vijayakumar, Y. Kashter, R. Kelner, and J. Rosen, "Coded aperture correlation holography system with improved performance [Invited]," Appl. Opt. **56**(13), F67–F77 (2017).
21. A. Vijayakumar and J. Rosen, "Spectrum and space resolved 4D imaging by coded aperture correlation holography (COACH) with diffractive objective lens," Opt. Lett. **42**(5), 947–950 (2017).
22. W. Chi and N. George, "Optical imaging with phase-coded aperture," Opt. Express **19**(5), 4294–4300 (2011).
23. A. Levin, R. Fergus, F. Durand, and W. T. Freeman, "Image and depth from a conventional camera with a coded aperture," ACM Trans. Graph. **26**(3), 70 (2007).
24. C. Zhou, S. Lin, and S. Nayar, "Coded aperture pairs for depth from defocus," in 2009 IEEE 12th International Conference on Computer Vision (ICCV), 325–332 (2009).
25. H. Nagahara, C. Zhou, T. Watanabe, H. Ishiguro, and S. K. Nayar, "Programmable aperture camera using LCoS," in "Computer Vision–ECCV 2010," (Springer, 2010), pp. 337–350.
26. A. Greengard, Y. Y. Schechner, and R. Piestun, "Depth from diffracted rotation," Opt. Lett. **31**(2), 181–183 (2006).
27. Y. Shechtman, S. J. Sahl, A. S. Backer, and W. E. Moerner, "Optimal point spread function design for 3D imaging," Phys. Rev. Lett. **113**(13), 133902 (2014).
28. A. S. Backer and W. E. Moerner, "Extending single-molecule microscopy using optical Fourier processing," J. Phys. Chem. B **118**(28), 8313–8329 (2014).
29. M. R. Hatzvi and Y. Y. Schechner, "Three-dimensional optical transfer of rotating beams," Opt. Lett. **37**(15), 3207–3209 (2012).
30. S. Jia, J. C. Vaughan, and X. Zhuang, "Isotropic three-dimensional super-resolution imaging with a self-bending point spread function," Nat. Photonics **8**(4), 302–306 (2014).
31. Y. Kashter and J. Rosen, "Enhanced-resolution using modified configuration of Fresnel incoherent holographic recorder with synthetic aperture," Opt. Express **22**(17), 20551–20565 (2014).
32. C. Liu, S. Knitter, Z. Cong, I. Sencan, H. Cao, and M. A. Choma, "High-speed line-field confocal holographic microscope for quantitative phase imaging," Opt. Express **24**(9), 9251–9265 (2016).
33. P. Bouchal and Z. Bouchal, "Selective edge enhancement in three-dimensional vortex imaging with incoherent light," Opt. Lett. **37**(14), 2949–2951 (2012).
34. D. J. Goldstein, *Understanding the light microscope: A computer aided introduction* (Academic, 1999) Chap.1.
35. R. W. Gerchberg and W. O. Saxton, "A practical algorithm for the determination of phase from image and diffraction plane pictures," Optik (Stuttg.) **35**(2), 227–246 (1972).
36. G. Z. Yang, B. Z. Dong, B. Y. Gu, J. Y. Zhuang, and O. K. Ersoy, "Gerchberg-Saxton and Yang-Gu algorithms for phase retrieval in a nonunitary transform system: a comparison," Appl. Opt. **33**(2), 209–218 (1994).

1. Introduction

Indirect imaging by incoherent digital holography [1–5] can provide satisfactory solutions to several technological problems of imaging. Two-wave interference is commonly involved in the process of recording incoherent digital holograms. In general, the terms 'interference' and 'holography' are inseparable as the former is needed for the latter in many situations [6]. The phenomenon of interference is a necessity in most of the holographic systems in order to lock the phase information of the object. With interference becoming necessary, sophisticated optical setups with vibration isolation systems and time-consuming optical alignment procedures are becoming unavoidable. Moreover, higher optical power is usually needed to compensate the loss due to beam splitting, and a special care is sometimes required to equalize the power of the interfering beams, in order to obtain high fringe visibility. The above drawbacks, arising from the interference requirement, have motivated researchers to

Optics EXPRESS

develop simpler, but equally capable and sometimes better, interferenceless holography techniques [7,8].

The origin of the present work is related to an interference-based incoherent digital holography system called Fresnel incoherent correlation holography (FINCH) [9,10]. FINCH has demonstrated lateral resolving capabilities beyond the resolution limit dictated by the classical Lagrange invariant conditions [11–14]. The non-classical lateral resolution feature of FINCH arising from the self-interference phenomenon has been adapted well into other well-established resolution enhancement techniques such as structured illumination to obtain super-resolution [15]. A disadvantage of the self-interference holography is the high focal depth, or in other words, low axial resolution of the reconstructed images [13]. As a consequence, when a particular plane of a three-dimensional (3D) object is reconstructed, the information of the other planes is strongly present as defocus noise. Different techniques have been developed in the recent years to improve the axial resolution of FINCH [16–18].

Recently, a self-interference incoherent digital holography technique called coded aperture correlation holography (COACH) was developed with an axial resolution higher, but with a lateral resolution lower, than that of FINCH [19]. On the other hand, the lateral and the axial resolutions of COACH were found to be similar to that of equivalent regular imaging systems. A drawback of COACH is the background noise present in the reconstructed images. Different noise reduction techniques have been developed in order to enhance the performance of COACH and to achieve an optimal signal to noise ratio (SNR) [20]. The four-dimensional imaging capabilities of COACH in three spatial dimensions and wavelength have been reported recently [21]. COACH was born as an improved version of FINCH and in some sense COACH is a generalization of FINCH. In both methods, the light from each object point is split into two mutually coherent beams, whereas only one of the beams is modulated by a coded phase mask (CPM) [See Fig. 1(a) and 1(b)]. In both cases, the modulated and unmodulated beams are interfered, such that the obtained interference pattern is a hologram containing the information about the 3D location of the object point. The main difference between COACH and FINCH is the CPM, while in FINCH the CPM is a two-dimensional (2D) quadratic phase function, in COACH the CPM is a quasi-random phase function.

This study is one step beyond COACH, where a new incoherent digital holography COACH-based technique is introduced and demonstrated. However, in contrast to COACH, the hologram recording is done without using two-wave interference. The new method is termed interferenceless coded aperture correlation holography (I-COACH), and it is capable of recording and reconstructing 3D information of incoherently illuminated objects. Using I-COACH, the 3D scene can be recorded and stored onto a 2D hologram without using laser light, without using wave interference, without changing the viewpoint of the recorder, without moving any part of the system and without measuring the depth of any part of the scene prior to the hologram acquisition.

A comparative view of the three holographic systems is presented in Fig. 1, whereas Fig. 1(a), 1(b) and 1(c) describe schematically the FINCH, COACH and I-COACH systems, respectively. All the three systems use three camera shots to create the digital hologram, and in all cases, the hologram is reconstructed by a correlation with some impulse response function. However, I-COACH is the only setup, among these three, that does not use two-wave interference to record the hologram. Note that in FINCH the 3D location of any object point is encoded into the phase distribution at the sensor plane. Therefore, wave interference is essential to record this spatial information. In COACH, on the other hand, the 3D spatial information of a point is encoded into both the phase and the amplitude of the recorded optical signature. Wave interference reveals this complex function and stores it as a complex 2D digital hologram. The present study of I-COACH shows that the information in the phase is actually redundant. The point spatial information can be reconstructed to an image with the same qualities of the COACH image, from the intensity signature only, recorded without interference. In other words, I-COACH demonstrates that two-wave interference is not the

Optics EXPRESS

only option to record 3D information. Transferring a wavefront through several independent coded apertures, and recording the intensity without interference, can be an attractive alternative method for such a phase-to-intensity conversion.

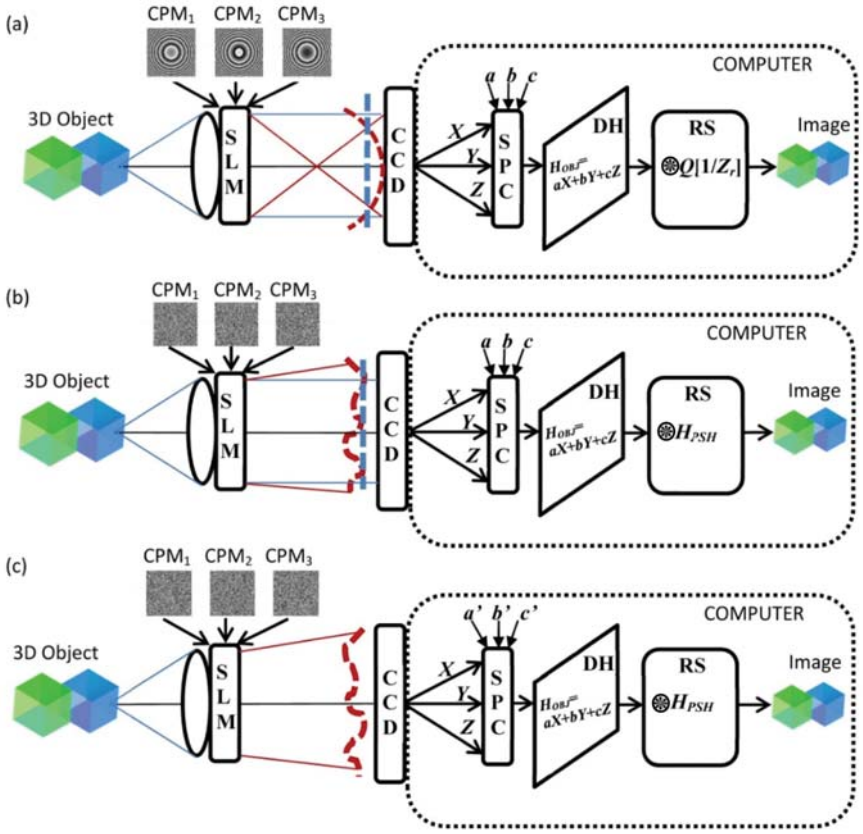

Fig. 1. Schemes of the three incoherent digital systems: (a) FINCH; (b) COACH; (c) I-COACH. The dashed blue and red lines are wave fronts. In FINCH and COACH the blue and the red waves interfere. In I-COACH there is only a single diffracted wave, and therefore there is no wave interference. CPM-coded phase mask, SLM-spatial light modulator, CCD-charge coupled device, SPC-superposition calculator, DH-digital hologram, RS-reconstruction system, X, Y, Z-Intensity pattern recorded by the CCD in three camera shots, a, b, c-complex constants, H_{OBJ}-complex digital object hologram, H_{PSH}-point spread hologram, $\circledast$ - correlation sign, $Q(1/z_r)=\exp\left[i\pi\left(z_r\lambda\right)^{-1}\left(x^2+y^2\right)\right]$.

Imaging with a phase coded aperture has already been proposed by Chi and George [22]. However, Chi and George avoided from recording a digital hologram of a 3D scene and their results have suffered from high level of background noise because of lack of any noise reduction mechanism. Binary coded apertures have been used in [23–25], but not for recording digital holograms of the 3D observed scene. Part of this study deals with PSF engineering for 3D imaging as in [26–30], but I-COACH is more than a regular 3D imaging with or without PSF engineering. In I-COACH, the entire 3D visual data is compressed into a 2D hologram, a benefit which enables easier storing, transferring, or processing the data. In contrast to FINCH and COACH, in I-COACH this advantage has been achieved without two-wave interference. Digital holograms are important in the imaging technology because they are used as a compressed storing medium in which 3D information is stored into a 2D digital

Optics EXPRESS

matrix. Furthermore, digital holograms can be composed together to a hologram with a large synthetic aperture [31], they can be used for imaging objects covered by a scattering medium [4] and they can be processed to yield various 2D sections of a 3D image [32], or edge-enhanced images [33].

2. Methodology

The original COACH [19] is based on the principle that each object point creates on the sensor plane the same complex-valued signature function shifted laterally according to the lateral location of the object point. Denoting the complex valued signature function as a point spread hologram (PSH), one can conclude that the object hologram is a collection of the same PSHs, each of which is located laterally according to the shape of the object. The PSH is recorded prior to the recording process of the object hologram. Once the complex hologram of the object is recorded into the computer, the image of the object can be reconstructed by a cross-correlation between the object hologram and the PSH. The 3D imaging capability is achieved because the points distributed along the z-axis induce different uncorrelated PSHs. To avoid high background bias and to minimize the noise in the cross-correlation, the object hologram and the PSH should be complex valued, random-like functions. However, since the hologram are recorded by a digital camera which measures only real positive intensity signals, the interference with the phase-shift procedure are needed to create the complex-valued holograms. Nevertheless, in this study, we show that because of the random-like nature of the PSH, neither the interference nor the phase-shift procedure is really essential. This work shows that I-COACH offers an alternative process without two-wave interference, which takes the same time, needs the same number of exposures and yields similar results as COACH. Apparently, if the digital camera records three random-like independent intensity distributions, they can all be projected to the complex space and yield complex-valued PSH with the same properties obtained by the wave interference process of COACH.

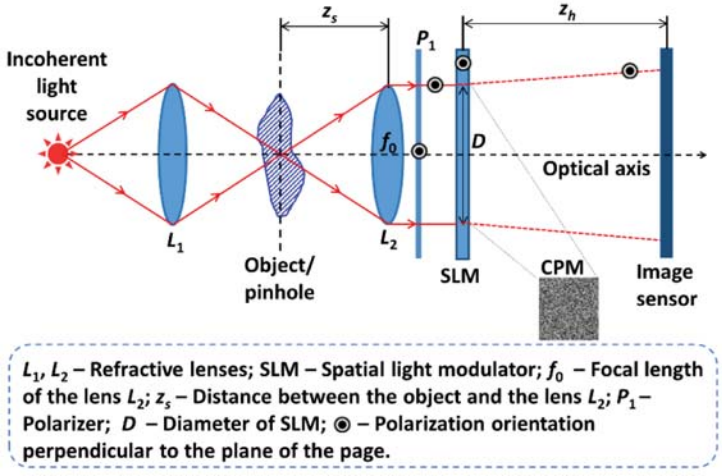

Fig. 2. Optical configuration of I-COACH for recording object and PSHs.

The optical configuration of I-COACH is shown in Fig. 2. Light from an incoherent source is focused using lens L_1 to critically illuminate a point object [34]. The light diffracted from the point object is collected and collimated by lens L_2, located at a distance z_s from the point object. The light collimated by L_2 is polarized by polarizer P_1 along the active axis of the spatial light modulator (SLM) such that most of the light incident on the SLM is modulated by the phase mask displayed on the SLM. The mask on the SLM is a random-like CPM calculated using Gerchberg-Saxton algorithm (GSA) [35,36] under the constraint that its spectrum is a pure-phase function, similar to [19] i.e., the intensities are constrained to be

Optics EXPRESS

uniform and equal to 1 in both the SLM and its spectrum domains. Note that in the GSA of [19] only a single CPM is created where the other two CPMs of COACH are phase-shifted versions of this single CPM. On the other hand, in I-COACH three independent CPMs are created by initiating the algorithm with three different phase-only random CPMs. The constraint of a uniform intensity in the spectrum reduces the side lobes of the autocorrelation peaks of the PSH and therefore the background noise of the reconstructed images is less severe than with other constraints. The light diffracted by the CPM is recorded by an image sensor located at a distance of z_h from the SLM. The experiment is repeated by moving the point object to different axial locations and recording the corresponding intensity patterns to create the PSH library for the various z locations. Once the PSH library is ready for use in the computer, the training stage of the system is completed and the system is ready to record and to reconstruct holograms of general 3D objects. An object placed within the axial boundaries of the PSH library should be recorded using the same CPMs used for the PSH library. The object information at different axial planes can be reconstructed by correlating the object hologram with the elements of the PSH library recorded at the corresponding axial planes. In this way, the information at different depths of an object can be effectively demultiplexed.

At first glance, the setup of I-COACH looks similar to the COACH system [19,20], but they are actually different. The COACH is a self-reference interferometer and as so it has a mechanism of splitting the beams by a polarizer in front of the SLM and a mechanism for combining the beams by a second polarizer behind the SLM. In order to get an interference pattern with high fringe visibility, one should use a light source with a narrow bandwidth to guarantee that the maximal path difference between the interferometer channels is shorter than the coherence distance. Moreover, in order to eliminate the bias term and the twin image from the hologram one should use the phase-shift process. All these constraints do not exist in I-COACH. Although there is one polarizer in front of the SLM, it does not split the beam and it can be removed if the SLM modulate light polarized in all orientations.

Based on Fig. 2, in the case of a point object with the amplitude $\sqrt{I_s}$ located at $(\bar{r}_s, z_s) = (x_s, y_s, z_s)$, light diffracted from the object reaches the lens L_2 with a complex amplitude $\sqrt{I_s}\, C_1 L(\bar{r}_s / z_s)\, Q(1/z_s)$, where Q and L represent quadratic and linear phase functions, given by $Q(a) = \exp\left[i\pi a \lambda^{-1}\left(x^2 + y^2\right)\right]$ and $L(\bar{s}/z) = \exp\left[i2\pi(\lambda z)^{-1}\left(s_x x + s_y y\right)\right]$ respectively, and C_1 is a complex constant. The complex amplitude immediately after lens L_2 is given as $\sqrt{I_s}\, C_1 L(\bar{r}_s / z_s) \cdot Q(1/z_s) \cdot Q(-1/f_0)$. Assuming that the distance between the lens L_2 and the SLM is negligible, the complex amplitude after SLM is given by $\sqrt{I_s}\, C_1 L(\bar{r}_s / z_s) \cdot Q(1/z_s) \cdot Q(-1/f_0) \exp\left[i\Phi_k(\bar{r})\right]$, where $\Phi_k(\bar{r})$ is the k-th quasi-random phase CPM calculated using the GSA. The reason for using K different CPMs is clarified in the following. The light diffracted from the SLM propagates by a distance of z_h before it reaches the image sensor. The complex amplitude at the image sensor is given as a convolution of $\sqrt{I_s}\, C_1 L(\bar{r}_s / z_s) \cdot Q(1/z_s) \cdot Q(-1/f_0) \cdot \exp\left[i\Phi_k(\bar{r})\right]$ with $Q(1/z_h)$. Therefore, the intensity pattern on the image sensor is given by,

$$I_k(\bar{r}_0; \bar{r}_s, z_s) = \left| \sqrt{I_s} C_1 Q\left(\frac{1}{z_s}\right) L\left(\frac{\bar{r}_s}{z_s}\right) Q\left(-\frac{1}{f_0}\right) \exp\left[i\Phi_k(\bar{r})\right] * Q\left(\frac{1}{z_h}\right) \right|^2, \qquad (1)$$

where the asterisk sign denotes a two-dimensional convolution and $\bar{r}_0 = (u, v)$ is the transverse location vector on the sensor plane. Equation (1) can be simplified as

Optics EXPRESS

$$I_k\left(\bar{r}_0;\bar{r}_s,z_s\right)=\left|\sqrt{I_s}C_1L\left(\frac{\bar{r}_s}{z_s}\right)Q\left(\frac{1}{z_1}\right)\exp\left[i\Phi_k\left(\bar{r}\right)\right]*Q\left(\frac{1}{z_h}\right)\right|^2=I_k\left(\bar{r}_0-\frac{z_h}{z_s}\bar{r}_s;0,z_s\right), \quad (2)$$

where $z_1 = z_s f_0/(f_0-z_s)$. The last equality of Eq. (2) indicates that the intensity on the sensor plane is a shifted version of the intensity response for a point object located on the optical axis $\left(\bar{r}_s=0\right)$, where the distance of the shift is $\bar{r}_s\, z_h/z_s$. The intensity response for centered object points is used as the k-th component of the PSH, as described in the following.

A 2D object at some distance z_s from the lens L_2 can be considered as a collection of N uncorrelated point objects given by

$$o\left(\bar{r}_s\right)=\sum_j^N a_j\delta\left(\bar{r}-\bar{r}_{s,j}\right). \quad (3)$$

Assume that the object is illuminated by an incoherent quasi-monochromatic light source. The response of the system to a single object point is given by Eq. (2), and since there is no interference between the responses, due to the spatial incoherence of the object light, the overall intensity distribution on the sensor plane is a sum of the point responses, given by,

$$I_{OBJ,k}\left(\bar{r}_0;z_s\right)=\sum_j a_j I_k\left(\bar{r}_0-\frac{z_h}{z_s}\bar{r}_{s,j};0,z_s\right). \quad (4)$$

$I_{OBJ,k}\left(\bar{r}_0;z_s\right)$ and $I_k\left(\bar{r}_0;z_s\right)$ are both positive real quasi-random functions but, in general, a cross-correlation between them yields an undesired background distribution. In order to avoid this background distribution both $I_{OBJ,k}\left(\bar{r}_0;z_s\right)$ and $I_k\left(\bar{r}_0;z_s\right)$ are projected onto the complex domain as follows,

$$H_{PSH}\left(\bar{r}_0;z_s\right)=\sum_{k=1}^K I_k\left(\bar{r}_0;z_s\right)\exp\left(i\theta_k\right). \quad (5a)$$

and

$$\begin{aligned}H_{OBJ}\left(\bar{r}_0;z_s\right)&=\sum_{k=1}^K I_{OBJ,k}\left(\bar{r}_0;z_s\right)\exp\left(i\theta_k\right)\\&=\sum_{k=1}^K\sum_j a_j I_k\left(\bar{r}_0-\frac{z_h}{z_s}\bar{r}_{s,j};0,z_s\right)\exp\left(i\theta_k\right).\\&=\sum_j a_j H_{PSH}\left(\bar{r}_0-\frac{z_h}{z_s}\bar{r}_{s,j};z_s\right),\end{aligned} \quad (5b)$$

where $H_{PSH}\left(\bar{r}_0;z_s\right)$ and $H_{OBJ}\left(\bar{r}_0;z_s\right)$ are the PSH and the object holograms, respectively. It should be noted that in order to minimize the background noise, the autocorrelation of the PSH should be as close as possible to a delta function. Based on the convolution theorem, this condition is satisfied if the magnitude of the Fourier transform of the PSH is uniform over the entire spectrum domain. This condition is partially achieved by the spectral constraint of the GSA. In order to satisfy the spectral constraint of the GSA it is enough to choose $K = 2$ and $|\theta_1-\theta_2| = \pi$ (assuming the average of all the involved intensities is the same). However, to obtain complex holograms that are similar to the original COACH holograms [19], we choose three angles of projection ($K = 3$) as following: $\theta_1 = 0$, $\theta_2 = 2\pi/3$, $\theta_3 = 4\pi/3$. Note that in the case of $K = 2$ mentioned above, the detected intensities are projected on the real axis, while in the second case of $K = 3$, the detected intensities are projected onto the entire complex domain. Therefore, there are more degrees of freedom in the second case and hence with this

Optics EXPRESS

kind of projection, the reconstruction process is expected to yield less background noise than in the first case. This last conclusion was confirmed by comparative simulation experiments.

The image is reconstructed by correlating $H_{OBJ}(\overline{r}_0;z_s)$ with $H_{PSH}(\overline{r}_0;z_s)$ as follows,

$$\begin{aligned} P(\overline{r}_R) &= \iint H_{OBJ}(\overline{r}_0;z_s)\,H^*_{PSH}(\overline{r}_0-\overline{r}_R;z_s)\,d\overline{r}_0 \\ &= \iint \sum_j a_j H_{PSH}\left(\overline{r}_0-\frac{z_h}{z_s}\overline{r}_{s,j};z_s\right) H^*_{PSH}(\overline{r}_0-\overline{r}_R;z_s)\,d\overline{r}_0. \\ &= \sum_j a_j \Lambda\left(\overline{r}_R-\frac{z_h}{z_s}\overline{r}_{s,j}\right) \approx o\left(\frac{\overline{r}_s}{M_T}\right). \end{aligned} \tag{6}$$

where Λ is a δ-like function, approximately equal to 1 around (0,0) and to small negligible values elsewhere. It must be noted that when a H_{PSH} from the library is correlated with H_{OBJ}, only the object image corresponding to the axial plane of H_{PSH} is reconstructed. The final result of Eq. (6), the reconstructed image, is a magnified image of the object, with a transverse magnification of $M_T = z_h/z_s$. Since the image is reconstructed using correlation [Eq. (6)], the transverse and axial resolutions are dictated by the transverse and axial correlation lengths, determined by the width and the length of the smallest spot that can be recorded on the sensor plane by the SLM with an active area of diameter of D (assuming that the active area is the smallest aperture in the system). Therefore, the transverse and axial resolutions are approximately $1.22\lambda z_s/D$ and $8\lambda(z_s/D)^2$ respectively, matching with the resolution values of the regular incoherent imaging system with a similar numerical aperture (NA). The method of cross-correlation expressed by Eq. (6) may not be the only, or the optimal, way to reconstruct the image of the original object. However, it is the most reasonable way for this preliminary study, since the cross-correlation has been successful for 3D imaging with the interference-based methods FINCH and COACH.

I-COACH has the unique capability of storing 3D information in a single 2D hologram recorded without wave interference, but the optical configuration has the simplicity of a regular imaging system. It should be noted that any two object points along the optical axis separated from each other by a distance longer than the axial correlation length, create two uncorrelated PSHs. Because of this property, the 3D reconstruction from the 2D hologram is enabled.

3. Experiments

The characteristics of I-COACH are experimentally studied using a digital holographic setup shown in Fig. 3. The setup consists of two illumination channels and two identical light emitting diodes (LEDs) (Thorlabs LED631E, 4 mW, λ = 635 nm, $\Delta\lambda$ = 10 nm) which are mounted on the two channels. It should be emphasized that the two channels never laterally overlap and therefore, the beams from these channels never interfere. The light emitted by the two LEDs is collected by two identical objective lenses L_{1A} and L_{1B} to critically illuminate the objects mounted in the two channels [19]. The objects are mounted at a distance of 3 cm from lenses L_{1A} and L_{1B}. The light diffracted by the two objects are combined using a beam splitter BS_1 and collimated by a lens L_2 with a diameter of 2.5 cm and a focal length f_0 = 20 cm resulting in an NA of ~0.063. Therefore, the lateral and axial resolutions are approximately 6.1 μm (0.61λ/NA) and 0.32 mm [2λ/(NA)^2], respectively. The collimated light passes through a polarizer P_1 and is incident on an SLM (Holoeye PLUTO, 1920 × 1080 pixels, 8 μm pixel pitch, phase-only modulation) which is mounted at a distance of 20 cm from the lens L_2. The polarizer P_1 is oriented along the direction of the active axis of the SLM to enable full modulation of the incident light. On the SLM, the CPMs designed using GSA are displayed one after the other to record the corresponding K = 3 intensity patterns at the image sensor (Hamamatsu ORCA-Flash4.0 V2 Digital CMOS, 2048 × 2048 pixels, 6.5 μm pixel pitch,

Optics EXPRESS

monochrome) which is mounted at a distance of Z_h = 40 cm from the SLM. In order not to reduce the image resolution below the limit determined by the NA of the system, the most peripheral rays should be able to meet on the image detector. For an SLM pixel size of Δ, SLM radius R and central wavelength λ, the minimal Z_h which guarantees that the resolution is not reduced below the standard limit of 0.61λ/NA is $Z_{h,min} = 2\Delta \cdot R/\lambda$. For the parameters of the current experiment $Z_{h,min}$ is about 13 cm.

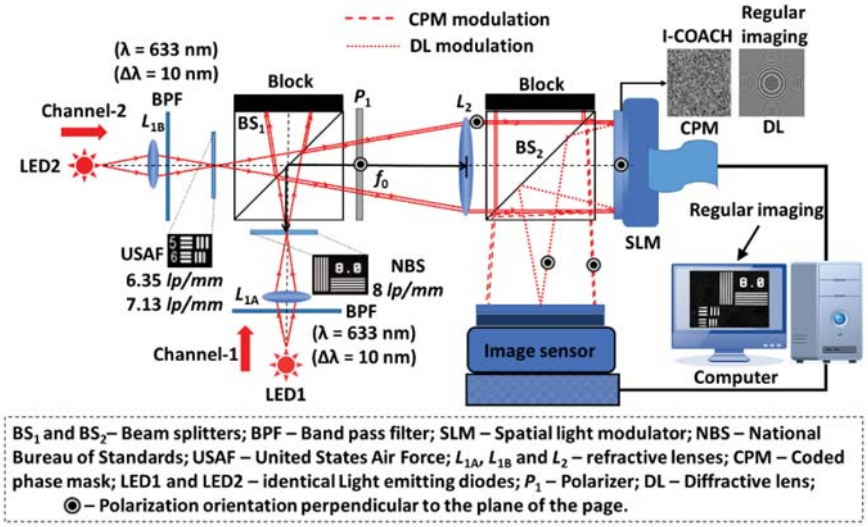

Fig. 3. Experimental setup of I-COACH with two illumination channels. There is no time overlap between the two types of modulation, and there is no spatial overlap between the two channels. Therefore, there is never two-wave interference in this experiment.

To understand the features of I-COACH, various experiments were carried out with the experimental setup shown in Fig. 3. In the first experiment, a negative National Bureau of Standards chart (NBS) (NBS 1963A Thorlabs) was mounted on channel 1 and a pinhole with a diameter of 25 μm was mounted on channel 2, both at the front focal plane of the lens L_2. Three intensity patterns for the pinhole and three intensity patterns for the element of 8 lines per mm (*lp/mm*) on the NBS object were recorded, corresponding to the three independent CPMs displayed on the SLM, by blocking the respective channels. The three intensity patterns of the pinhole and the object were projected into the complex space with phase values $\theta = 0, 2\pi/3$ and $4\pi/3$, in order to generate the complex holograms for the pinhole and the object, respectively. The image of the object was reconstructed by a correlation of the two complex holograms H_{OBJ} and H_{PSH}. The phase images of the three CPMs calculated using GSA are shown in Figs. 4(a)-4(c). The intensity patterns recorded using the three CPMs for the pinhole and the NBS object are shown in Figs. 4(d)-4(f) and Figs. 4(g)-4(i), respectively. The phase of the synthesized complex PSH and object hologram are shown in Fig. 4(j) and 4(k), respectively. The magnitude of the synthesized complex PSH and object hologram are shown in Fig. 4(l) and 4(m), respectively. The reconstructed image is shown in Fig. 4(n) with a background noise (SNR = 5) which has been thoroughly studied in [20]. A phase-only filtering technique was employed during reconstruction to improve the SNR similar to [20] and the resulting reconstructed image (SNR = 16.7) is shown in Fig. 4(o). An image of the object was captured on the image sensor by displaying on the SLM a diffractive lens with a focal length of 40 cm, and the recorded image is shown in Fig. 4(p).

Optics EXPRESS

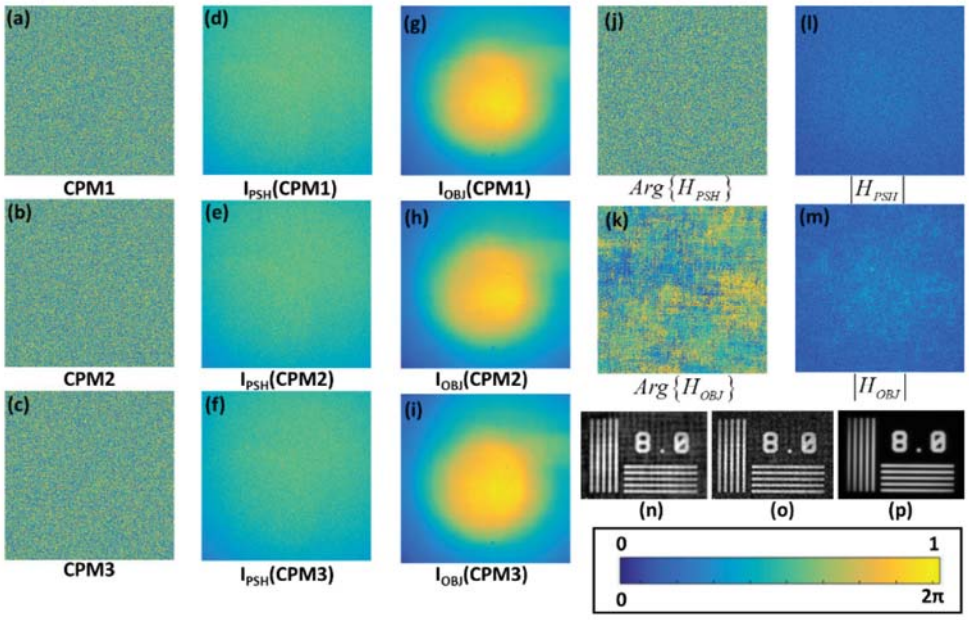

Fig. 4. Coded phase masks (a) CPM1, (b) CPM2, and (c) CPM3; Intensity patterns recorded using the CPMs for the pinhole (d) I_{PSH}(CPM1), (e) I_{PSH}(CPM2), and (f) I_{PSH}(CPM3); Intensity patterns recorded using the CPMs for the object (g) I_{OBJ}(CPM1), (h) I_{OBJ}(CPM2), and (i) I_{OBJ}(CPM3); (j) Phase and (l) magnitude of the synthesized H_{PSH}; (k) Phase and (m) magnitude of the synthesized H_{OBJ}; Reconstruction results of the NBS object with (n) matched filter (SNR = 5), (o) phase-only filter (SNR = 16.7) and (p) regular imaging of the NBS object.

In the second experiment, the axial resolution of I-COACH was studied using a pinhole with a diameter of 25 μm in one of the channels and blocking the other channel. In I-COACH, since the reconstruction is carried out using correlation, the axial resolution is given by the axial correlation length, which in the object plane, is same as the axial resolution of regular imaging [19]. For an SLM with an aperture of diameter D, the axial correlation length is given using scalar diffraction theory as $8\lambda(z_h/D)^2$. Since the axial magnification is $M_L = (z_h/z_s)^2$, the axial resolution in the object plane, can be given by $8\lambda(z_s/D)^2$ which is equivalent to the axial resolution $2\lambda/(\mathrm{NA})^2$ of a regular imaging system. The pinhole was initially placed at a distance of the focal length $z_s = f_0$ of the lens L_2 and three intensity patterns were recorded corresponding to the three CPMs displayed on the SLM and were projected onto the complex space. The experiment was repeated by varying the location of the pinhole from −25 mm to 25 mm with respect to the front focal plane of lens L_2 and the same three CPMs were displayed on the SLM. The corresponding three intensity patterns were recorded at the different axial locations. The resulting complex patterns were correlated with the PSH of $z_s = f_0$ and the reconstructed value at the center $(x,y) = (0,0)$ was measured for each axial location of the object. The experiment was repeated for regular imaging by displaying a diffractive lens with a focal distance of 40 cm to image the pinhole located at the front focal plane of the lens L_2 on the image sensor. The location of the pinhole was then varied from −25 mm to 25 mm with respect to the front focal plane of lens L_2 without changing the SLM mask, and the value at $(x,y) = (0,0)$ was measured for each axial location of the pinhole. The variation of the reconstructed and imaged central point for I-COACH and regular imaging are plotted with respect to the location of the pinhole in Fig. 5. The curve of Fig. 5 indicates that the axial resolution of both techniques is indeed approximately the same.

Optics EXPRESS

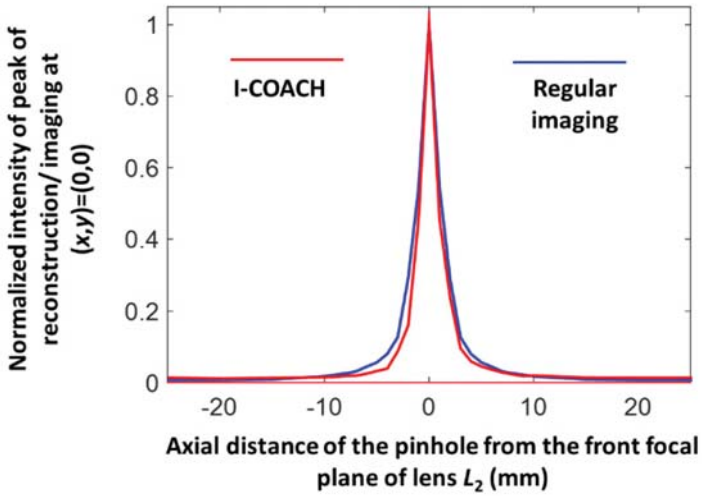

Fig. 5. Normalized intensity of reconstruction/imaging at $(x,y) = (0,0)$ versus the axial distance of the pinhole from the front focal plane of lens L_2.

In the third experiment, the three-dimensional imaging capability of I-COACH was studied by making use of both channels at the same time. In channel 1, an NBS object was mounted and a United States Air Force (USAF) chart (USAF 1951 1X Edmund Optics) was mounted on the second channel, both at the front focal plane of the lens L_2. The element 8 *lp/mm* was illuminated in the NBS object, while the elements 5 with 6.35 *lp/mm* and 6 with 7.13 *lp/mm* of Group 2 were illuminated in the USAF object. By varying the relative axial distance between the two objects, 3D objects with different thicknesses can be realized. The location of the NBS object was fixed, while the location of the USAF object was varied from −1 cm to 1 cm in steps of 0.5 cm from the front focal plane of the lens L_2. In every new location of the USAF, three intensity patterns were recorded and superposed into a complex hologram. The complex holograms were correlated with the PSHs recorded in the previous experiment using the phase-only filtering technique. The background noise was suppressed further by the averaging technique demonstrated in [20], which involves the recording of multiple intensity patterns by displaying independent CPMs and averaging over the synthesized complex correlation patterns. The reconstruction results of I-COACH after averaging over 20 different complex patterns and the results of regular imaging are shown in Fig. 6. The results indicate that the quality and the SNR of I-COACH are similar to that of regular imaging.

In the fourth experiment, the experimental setup shown in Fig. 7 was adjusted in order to image reflective 3D objects. Channel 2 was modified such that a 3D object can be illuminated critically by an illumination system from a perpendicular direction using the same beam splitter BS_1. The refractive lens L_{1B} used in this case is not identical to L_{1A} but with a focal length larger than that of L_{1B} in order to obtain a larger illumination area in the plane of the 3D objects. Three different objects were selected for the study: a LED, two one-cent coins separated by a distance and stapler pins. The experiment was carried out by recording three intensity patterns for every object. A correlation of the synthesized complex holograms with the PSH library was carried out to extract particular planar information from the objects. The reconstruction results of I-COACH after averaging over 20 samples were compared with regular imaging as shown in Figs. 8-10 for the LED, two one-cent coins, and stapler pins, respectively.

Optics EXPRESS

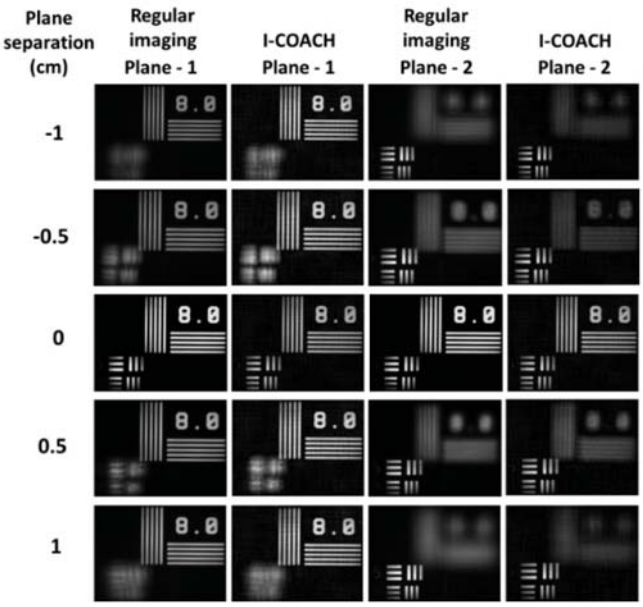

Fig. 6. Experimental comparison results of regular imaging and reconstruction of the I-COACH complex patterns at plane 1 (NBS chart) and plane 2 (USAF chart) of channels 1 and 2 respectively, when the plane separation was varied from -1 cm to 1 cm in steps of 0.5 cm.

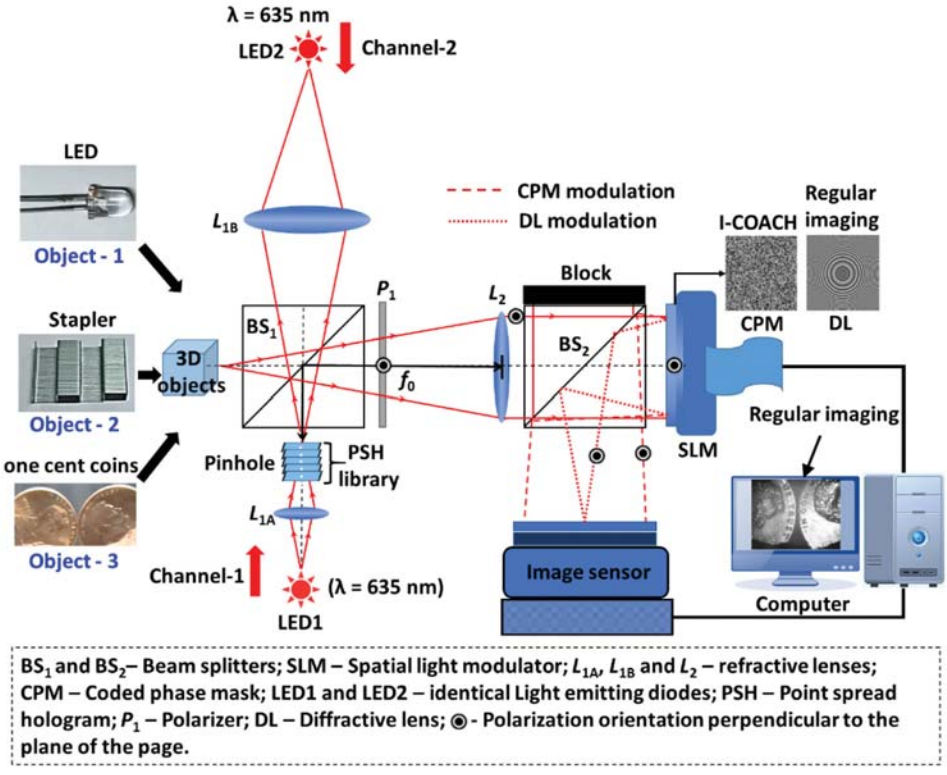

Fig. 7. Experimental setup of I-COACH with two illumination channels for studying reflective 3D objects.

Optics EXPRESS

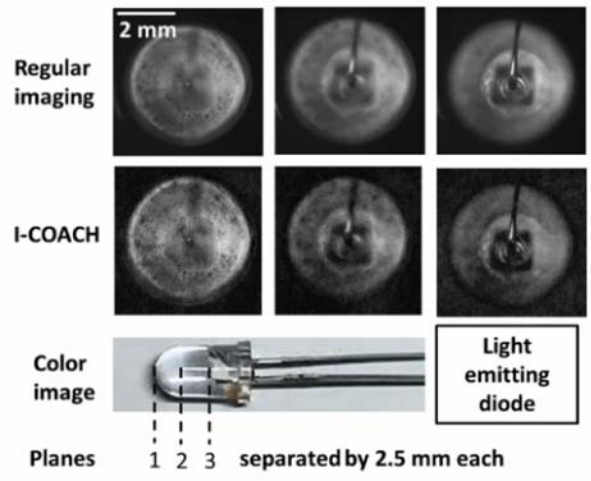

Fig. 8. Reconstruction and imaging results of I-COACH and regular imaging of the different planes of the LED.

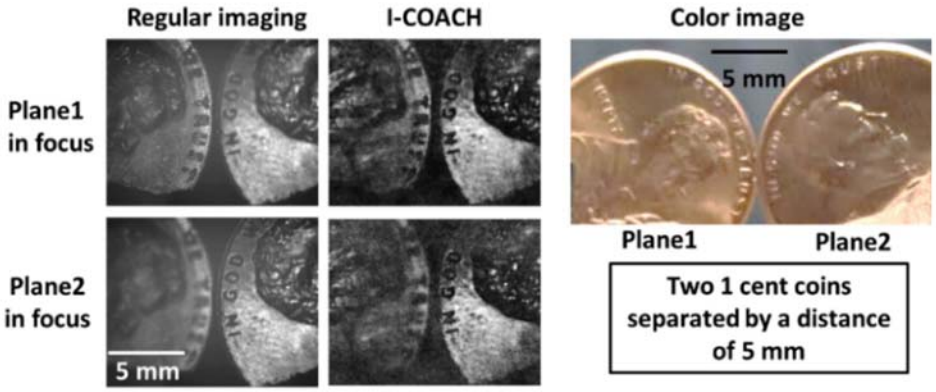

Fig. 9. Reconstruction and imaging results of I-COACH and regular imaging of the two planes of the two one-cent coins separated by a distance of 5 mm.

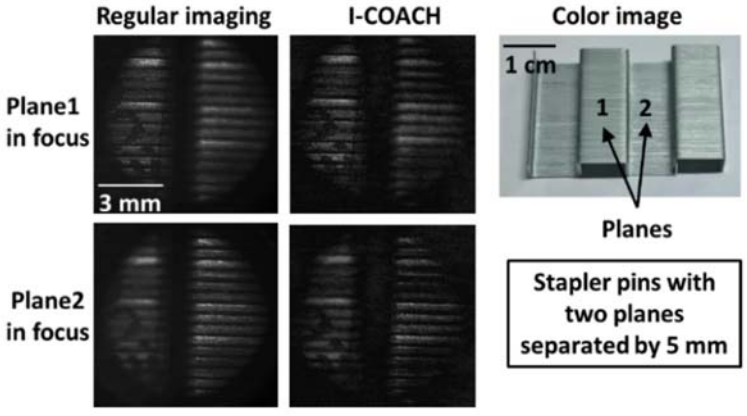

Fig. 10. Reconstruction and imaging results of I-COACH and regular imaging of the different planes of the stapler pins.

Optics EXPRESS

The reconstruction results of I-COACH at different planes after averaging is similar to that of regular imaging at the corresponding planes which demonstrate the capability of I-COACH. The comparison results confirm that the reconstruction results of I-COACH match accurately with regular imaging. In all the above experiments, objects which require only a limited field of view (FOV) have been selected and in some cases such as stapler pins and coins only a smaller area was illuminated in order to record and reconstruct all the information. For objects which require a larger FOV, an additional lens is necessary.

4. Summary and conclusions

We have developed an interferenceless holography technique called I-COACH for recording and reconstruction of 3D objects. The characteristics of I-COACH have been studied extensively and its lateral and axial resolutions were found to be similar to that of an equivalent regular imaging system. However, I-COACH has the capability of recording the entire 3D information by 2-3 camera shots and I-COACH can store the 3D visual information in a single 2D digital matrix. The 2D hologram of I-COACH has the complete 3D information of the object and the object image at any particular plane can be reconstructed by correlating the hologram with the PSH recorded in advance at that particular plane. These two capabilities of fast acquiring of 3D data and compressing the 3D data into 2D digital matrix are beyond the possibilities of regular imaging systems. In I-COACH, it is necessary to pre-record and create a PSH library at different axial locations. However, this process needs to be done only once, offline, as a part of training the system. Later, the PSH library can be used any number of times to reconstruct any 3D objects.

I-COACH has a simplified optical configuration in comparison to COACH and less optical power requirements. Therefore I-COACH can effectively replace existing cumbersome interference based holographic systems while yielding an uncompromising efficiency in studying 3D objects. The flexibility of the configuration can be utilized for easy integration of I-COACH into existing optical instruments for various applications. Finally, it should be noted that I-COACH also possesses encryption abilities similar to COACH due to the use of the CPMs i.e., only with the appropriate PSH keys, the object information at different axial planes can be decrypted.

Funding

Israel Science Foundation (ISF) (Grants No. 439/12, 1669/16).